

Research Article

Performance Analysis of Ti-Doped In_2O_3 Thin Films Prepared by Various Doping Concentrations Using RF Magnetron Sputtering for Light-Emitting Device

Wittawat Poonthong,¹ Narong Mungkung¹, Pakpoom Chansri,¹ Somchai Arunrungrusmi,¹ and Toshifumi Yuji²

¹Plasma and Electrical Discharge Laboratory, Department of Electrical Technology Education, King Mongkut's University of Technology Thonburi, Bangkok 10140, Thailand

²Faculty of Education, University of Miyazaki, Miyazaki, Japan

Correspondence should be addressed to Narong Mungkung; narong_kmutt@hotmail.com

Received 29 May 2020; Revised 13 July 2020; Accepted 3 August 2020; Published 28 August 2020

Academic Editor: Jinn Kong Sheu

Copyright © 2020 Wittawat Poonthong et al. This is an open access article distributed under the Creative Commons Attribution License, which permits unrestricted use, distribution, and reproduction in any medium, provided the original work is properly cited.

The influences of doping amounts of TiO_2 on the structure and electrical properties of In_2O_3 films were experimentally studied. In this study, titanium-doped indium oxide (ITiO) conductions were deposited on glass substrate by the dual-target-type radio frequency magnetron sputtering (RFS) system under different conditions of Ti-doped In_2O_3 targets, from Ti-0.5 wt% to Ti-5.0 wt%, along with 10 mTorr and 300 W pressure of RF power control that was used as a cost-effective transparent electrochemiluminescence (ECL) cell. From this process, the correlation between structural, optical, and electrical properties is reported. It was found that the best $1.14 \times 10^{-4} \Omega \text{cm}$ of resistivity was from Ti-2.5 wt% with the highest carrier concentration ($1.15 \times 10^{21} \text{ cm}^{-3}$), Hall mobility ($46.03 \text{ cm}^2/\text{V}\cdot\text{s}$), relatively transmittance (82%), and ECL efficiency ($0.43 \text{ lm}\cdot\text{W}^{-1}$) with well crystalline structured and smooth morphology. As a result, researchers can be responsible for preparing ITiO thin films with significantly improved microstructure and light intensity performance for the effectiveness of the display devices, as well as its simple process and high performance.

1. Introduction

The transparent conducting oxide (TCO) films have become of interest in the study of light-emitting materials because they have a high electrical conductivity and good transparency in the visible region. The potential application of TCO materials includes flat panel displays, electrooptical devices, and solar cells [1–4]. Particularly, electrochemiluminescence (ECL) has been developed due to their advantages (cost-effective manufacturing, simplified optical configuration, and high luminescence efficiency) and flexibility that can improve the light-emission performance of the application with the TCO devices [5, 6]. Among the conventional TCO films, indium tin oxide (ITO) films have been reported as TCO materials due to their good optical and electrical properties (resistivity about $10^{-4} \Omega \text{cm}$) [7, 8]. However, ITO materials are toxic

and they more often than not lack flexibility and thermal stability. To address these problems, a new alternative material to ITO was needed. In this sense, thin-film materials were developed with numerous channel materials incorporated with impurity doping such as Zn-doped In_2O_3 [9], Mo-doped In_2O_3 [8, 9], or Ti-In₂O₃ [10–12] that are found to be an ITO alternative for the transparent conducting application [13]. Titanium-doped indium oxide (ITiO) was considered the best choice because ITiO has a relatively low sheet resistance and demonstrates a high transmission in the near infrared (NIR), apart from its high mobility [10]. Many deposition techniques have been experimented in the preparation of ITiO thin films. Some of them are listed as pulsed laser deposition (PLD) [14], spray pyrolysis [15], ion beam sputtering [16], radio frequency (RF) magnetron sputtering [17], and chemical vapor deposition (CVD) [18]. Among the wide range of film

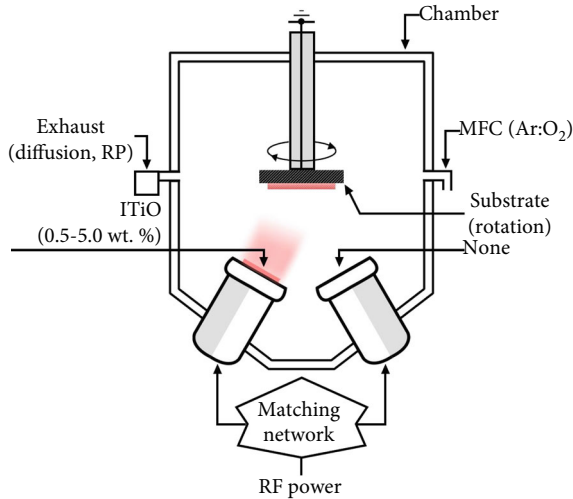


FIGURE 1: Schematic diagram of dual-target type by the radio frequency magnetron sputtering systems.

growth techniques, the RF magnetron sputtering technique is the most feasible and widely applicable to tailor stable and high-quality films that can provide a good film adhesion that is simple to prepare in a large area under a low deposition temperature. Previously, many groups have experimentally studied the deposition of quality ITiO films. Dong et al. [19] reported regarding the best optical transmittance of 70% to 90% by using DC magnetron sputtering at 300°C and titanium content of about 1.8 at%. Chaoumead et al. [20] used a 2.5 wt% TiO₂ and found out that the lowest resistivity was $1.2 \times 10^{-4} \Omega \text{ cm}$ and optical transmittance was 75% through an RF power of 300 W. Abe and Ishiyama [21] have reported the high Hall mobility of $82\text{--}90 \text{ cm}^2 \text{V}^{-1} \text{s}^{-1}$ and a low carrier density of $2.4\text{--}3.5 \times 10^{20} \text{ cm}^{-3}$ by using the DC magnetron sputtering method that was at 300°C. Consequently, in order to improve the possible application of the films as a transparent conducting electrode for electrooptical devices, the optical and electrical characteristics of the ITiO thin films should be studied.

In this study, we focus on the use of titanium-doped indium oxide (ITiO) that was deposited on glass substrate by using the RF magnetron sputtering method. The influence of doping concentration on the optical and electrical properties of conductive ITiO thin films was experimented in relation to their structural characterization. A further ECL cell was synthesized and applied with ITiO electrode to improve the efficiency of the ECL cells.

2. Materials and Methods

2.1. Preparation of ITiO Films. The preparation of titanium-doped indium oxide (ITiO) films was the same as in previous research [20]. In order to obtain good electrical properties, the ITiO films were deposited from a ceramic target that was experimentally used in the RF magnetron sputtering system. The targets were produced through the mixture of titanium dioxide (TiO₂; Sigma-Aldrich) and indium

oxide (In₂O₃; Sigma-Aldrich) with 99.99% of purity, and later, TiO₂ was doped at 0.5 wt% to 5.0 wt% in a weight and a step size of 0.5. The first step in the ceramic target production was to combine the TiO₂ and In₂O₃ by crushing these materials together with the aim of obtaining powder, which were then added to zirconia and ethanol and mixed. Afterwards, the mixture was ground by a spin grinding procedure in a chamber for 24 hours. Then, the ethanol was evaporated by rotating the heater until it was completely dried and thoroughly crushed, repeatedly in a mortar. Next, the ceramic targets were formed by the compression molding procedure into the size of 8.5 cm with a 1-ton force for 30 minutes. It was later sintered at 1400°C for 8 hours through the regular sintering process. In order to make the conductive ceramic target, the ceramics were scrubbed on one side to have a smooth surface, and coated with silver glue. At the end of the process, the targets were sintered at 600°C again. Finally, the IZO target with the resistivity of $895 \Omega \text{ cm}$, thickness of 0.7 cm, and diameter size of 8 cm were obtained.

2.2. The ITiO Film Deposition on Glass Substrate. The radio frequency magnetron sputtering (13.56 MHz) process was used for ITiO deposition in a $2.5 \text{ nm} \times 2.5 \text{ nm}$ size on glass substrates (Corning, NY, USA) [22–24]. To prepare the ITiO films for deposition, the glass substrate was cleaned ultrasonically in acetone and IPA (isopropanol) to remove any contaminations, residual solvents, or nonorganic components. In addition, 10 mTorr of working pressure was controlled during the deposition along with adjusting a pure Ar gas (99.99%) flow. The internal diameter of the stainless steel chamber was 350 nm. The target diameter was 75 nm, and the distance from the target to the substrate was 80 nm. The schematic diagram of two targets (ITO and Ti) was simultaneously sputtered on the radio frequency magnetron sputtering machine (YOUNGSIN-RF Co., Ltd.) as shown in Figure 1.

The chamber was pumped down to a base pressure (vacuum-exhausted) of 1×10^{-5} torr. Furthermore, 300°C of substrate temperature was kept during the deposition, and the RF power was controlled by 300 W for a total deposition time of 30 minutes. Additionally, the preparation of the ECL cell was the same as previous report [25] which consisted of ITiO glass/Ru(bpy)₃(PF₆)₂/ITiO glass.

2.3. Characteristic Method. The microstructure information of the film deposition on the glass substrate was studied by using an X-ray diffractometer (XRD) (Rigaku Co., D/max 2100H) under Cu K α irradiation ($\lambda = 1.5418 \text{ \AA}$); the atomic force microscopy (AFM) was used to investigate the ITiO film morphology. The particle morphology was measured by a field emission scanning electron microscope (FE-SEM). Moreover, the electrical properties like resistivity, carrier concentration, and Hall mobility were analyzed by a four-point probe (Dasol Eng., FPP-HS8). The optical properties of the ITiO films were measured through an UV spectrophotometer (Hitachi Co., U-3000) in a 300–800 nm range. The ECL device was measured by using a luminance meter

TABLE 1: The average roughness (R_{rms}) deposition condition of ITiO films.

Ti (wt%)	0.5	1.0	1.5	2.0	2.5	3.0	3.5	4.0	4.5	5.0
R_{rms} (nm)	15.915	13.889	11.730	10.872	5.676	11.264	11.370	15.248	18.926	19.287

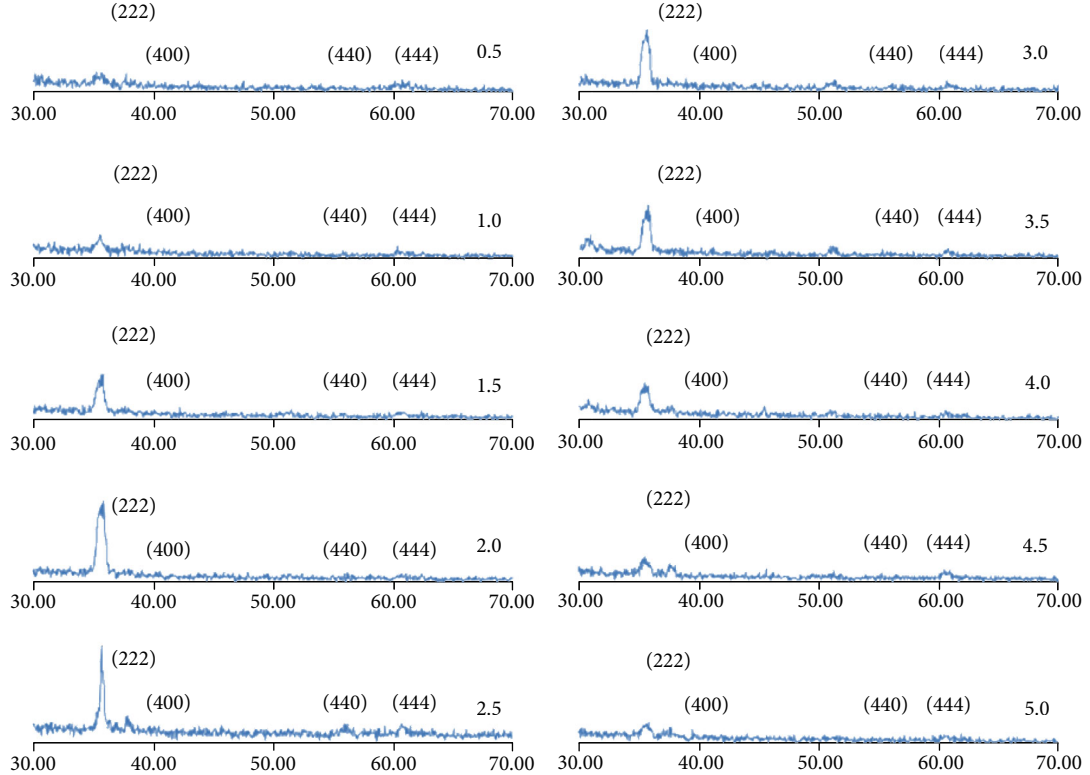


FIGURE 2: The XRD spectra of the ITiO films with various doping concentrations, deposited at 300 W of RF power.

(Konica Minolta: LS-150) under a 150 V and 400 Hz digital function generator (Hantek, HDG2012B).

3. Results and Discussion

3.1. Structural Properties. In order to perform a systematic study, the detailed analysis of ITiO films deposited on the glass substrate was controlled with the different variation of Ti-doped In_2O_3 target from 0.5 wt% to 5.0 wt% and 10 mTorr and 300 W of RF power working pressure. This process forms the scope of this study. In the first stage, the roughness parameter was carefully considered for an optical surface. Typically, surface roughness provides a light scattering and characterization surface. The roughness quality can be analyzed by reference [26], which was defined by the root mean square roughness (R_{rms}) of a standard deviation of the film surface height profile from the mean height. Therefore, R_{rms} is normally reported by the measurement of the surface roughness, as in

$$R_{\text{rms}} = \frac{1}{N} \sum_i^n (h_i - \langle h \rangle)^2, \quad (1)$$

where N is the number of image pixels, h_i is the height of the i

th pixel, and h is the mean height [27]. According to these conditions, Table 1 provides a comparison of the average roughness (R_{rms}) of this study to that of the ITiO films deposited on the glass substrate by the different Ti contents.

Figure 2 illustrates information regarding the XRD patterns of deposited ITiO films. As it can be seen, all samples show (222) diffraction peaks that indicate the formation of polycrystalline structure that is located around 36.55°. Looking at more details, the most intense diffraction peak was found in the increasing Ti-2.5 wt%. Therefore, the diffraction peak in the XRD spectrum was clearly caused by the (222) plane. However, the increasing Ti content may induce the formation of the TiO_2 particles that were deposited. In this case, it can retard the growth of In_2O_3 grain size.

The surface morphology of the ITiO films deposited on the glass substrate was investigated by the AFM analysis as shown in Figure 3. The AFM images, in Figure 3, presents the formation of granular structures and the variation of roughness by changing the Ti content from Ti-0.5 wt% to Ti-5.0 wt%. As it can be seen, when the Ti content is further increased, the surface roughness reduces, particularly, if the Ti-2.5 wt% sample value is lower than other Ti content due to the formation of the crystalline phase.

In Figure 4, the formation of well crystalline structure is presented, which shows SEM images of all deposited ITiO

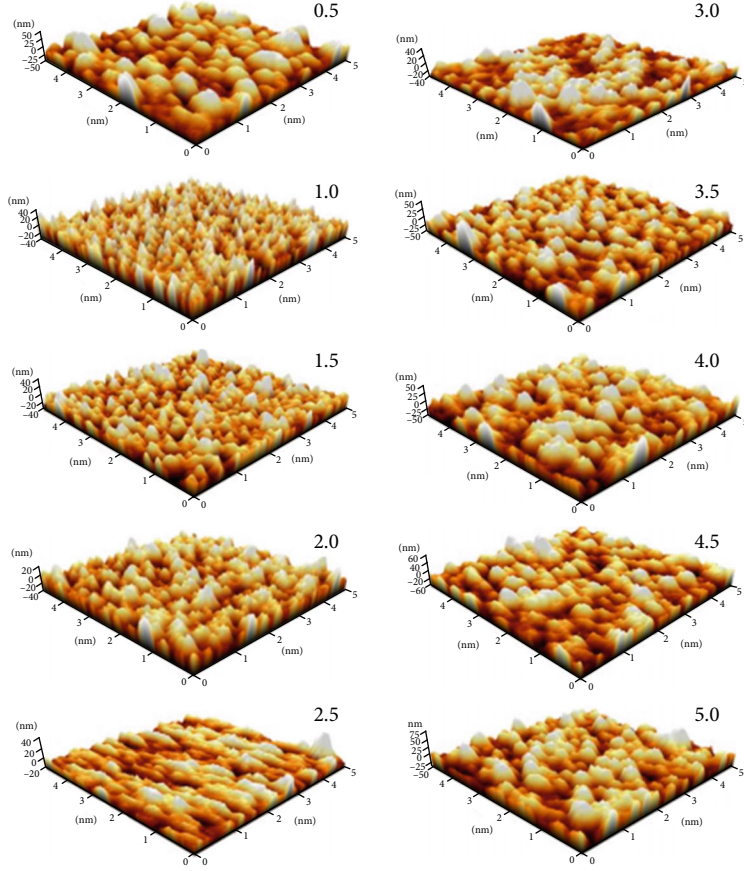


FIGURE 3: The surface morphology of ITiO films of different doping concentrations from Ti-0.5 wt% to Ti-5.0 wt%.

samples on glass substrates. The ITiO films deposited at all samples have triangular crystallites. As can be seen, from Ti-0.5 wt%-Ti-2.5 wt%, the size of these crystallites is decreased as the Ti doping concentration increases. The Ti-2.5 wt% sample illustrated the smoothest film surface, which leads to a greater concentration of grain size, obtaining as an area of films with low resistivity for electrons; therefore, the electrical performance is improved. On the other hand, from Ti-3.0 wt%-Ti-5.0 wt%, there has been a steady increase in crystallite and reduced density; this is due to the change of the crystal orientation as the Ti content increases.

3.2. Electrical Properties. As mentioned earlier, in Figure 2, the most XRD diffraction peak is displayed by Ti-2.5 wt%, and this affected the films' resistivity to the lowest. Therefore, as a further investigation, Figure 5 presents the information on electrical properties of the deposited ITiO films on the glass. Figure 5(a) shows the electrical resistivity of ITiO films. It was found that the significant point was shown at Ti-2.5 wt%, which obviously had the lowest resistivity point of $1.14 \times 10^{-4} \Omega \text{ cm}$. The reason for this result was due to the fact that at lowest resistivity, electron carrier can be easily moved from valence band to conductive band, leading to a high mobility and carrier concentration. As a result, the low-resistivity films were obtained. Generally, the resistivity was fluctuated dramatically. From the beginning of the

experiment, the resistivity starts very high with the Ti-0.5 wt% and then fell rapidly to hit to Ti-0.5 wt% and then rose steadily to the end of the graph. Note that these results are influenced by the films' properties when the Ti content was increased; the grain size also rose while the grain boundary was decreased. On the other hand, the carrier concentration in the plasma (ion or electron) density values are shown in Figure 5(b). Looking at the graph in more detail, we can see that the carrier concentration has reached the peak of around $1.15 \times 10^{21} \text{ cm}^{-3}$ under doping Ti-2.5 wt% which is then sharply reduced to the lowest point of approximately $8.635 \times 10^{21} \text{ cm}^{-3}$ under doping Ti-5.0 wt%. Likewise, when the number of carrier concentration is increasing, the ion plasma will have a high kinetic energy to move to the conduction band that affects the improvement in the Hall mobility value as shown in Figure 5(c). In Figure 5(c), we found that the highest mobility of $46.03 \text{ cm}^2/\text{V}\cdot\text{s}$ is shown by doping Ti-2.5 wt%, which is related to Figure 5(b). From these expressions, the lowest resistivity (Figure 5(a)) in Ti-2.5 wt% films is ascribed to four factors: the highest crystal structure having the most intense diffraction peak (Figure 2), the optimal doping concentration, the highest carrier concentration (Figure 5(b)), and the highest Hall mobility (Figure 5(c)). Regardless of the grain boundary scattering, the ions were easily transported inside the crystals; thus, the lowest resistivity of ITiO films was obtained.

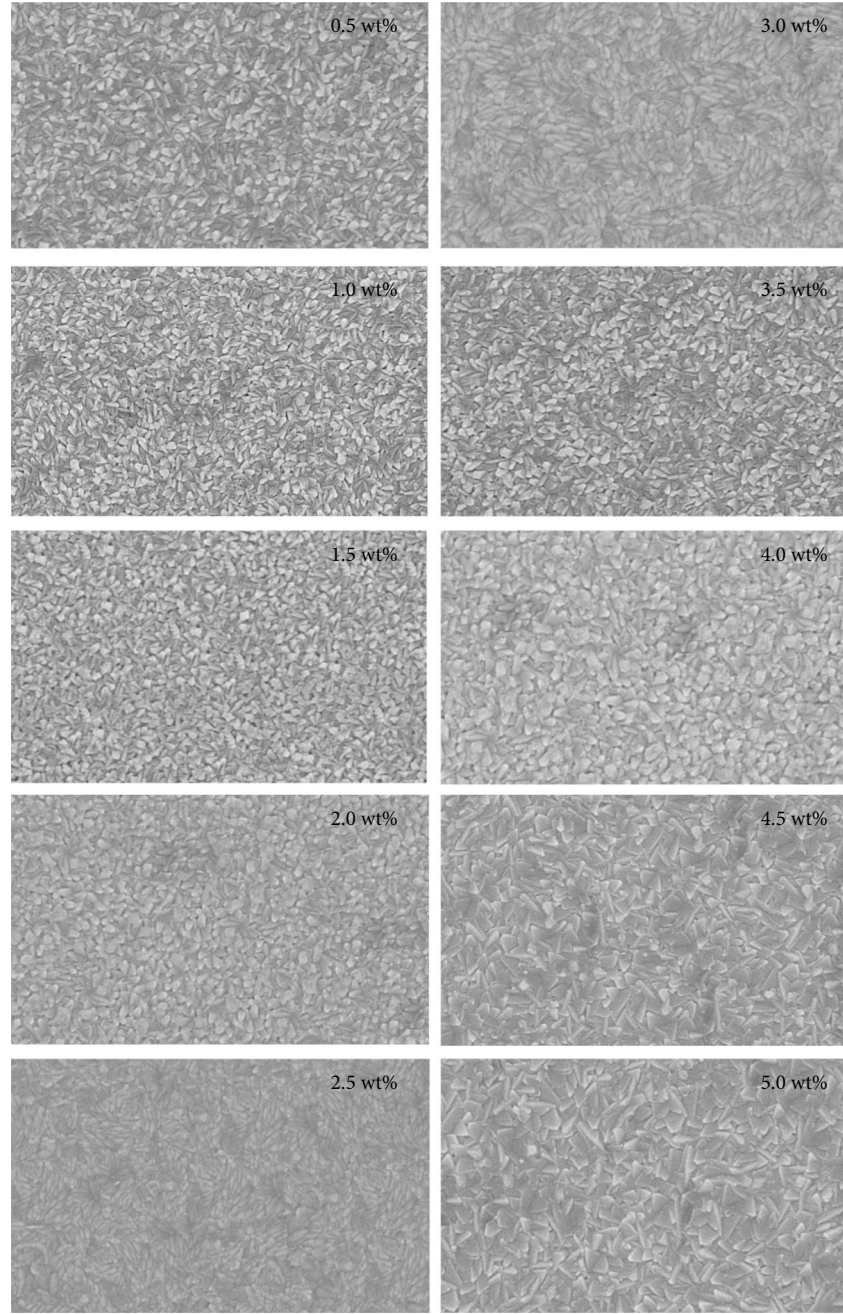


FIGURE 4: The SEM images of physical characteristics of ITiO films of different doping concentrations from Ti-0.5 wt% to Ti-5.0 wt%.

Table 2 provides a comparison of the electrical properties of this study to those of the films prepared by other deposition techniques. One can see that this study demonstrates a great potential in showing the lowest resistivity than that of the film prepared by other alternative methods.

Additionally, we investigated the optical transmittance spectra of ITiO films at various Ti doping concentrations as shown in Figure 6. The figure presents a comparative transmittance of the glass substrate. It can be seen that each transmittance spectrum has a steep absorption edge in the range of approximately 320 nm–360 nm and the average transmittance in the visible range between 400 nm and 800 nm. The Ti content of 2.5 wt% was particularly considered. The result

shows the transmittance was 82% with the industrial grade optical (Figure 5) and the required electrical property application for the transparent electrode [30].

In addition, the relationship between the photo energy (hv) and optical absorption coefficient (α) of ITiO films was investigated as shown in Figure 7. According to the equation [31–33], the optical band gap (E_g) is calculated based on

$$\alpha h\nu = A(h\nu - E_g)^{1/2}, \quad (2)$$

where α is the absorption coefficient, ν is the frequency of incident light, h is the Planck constant, and A is constant.

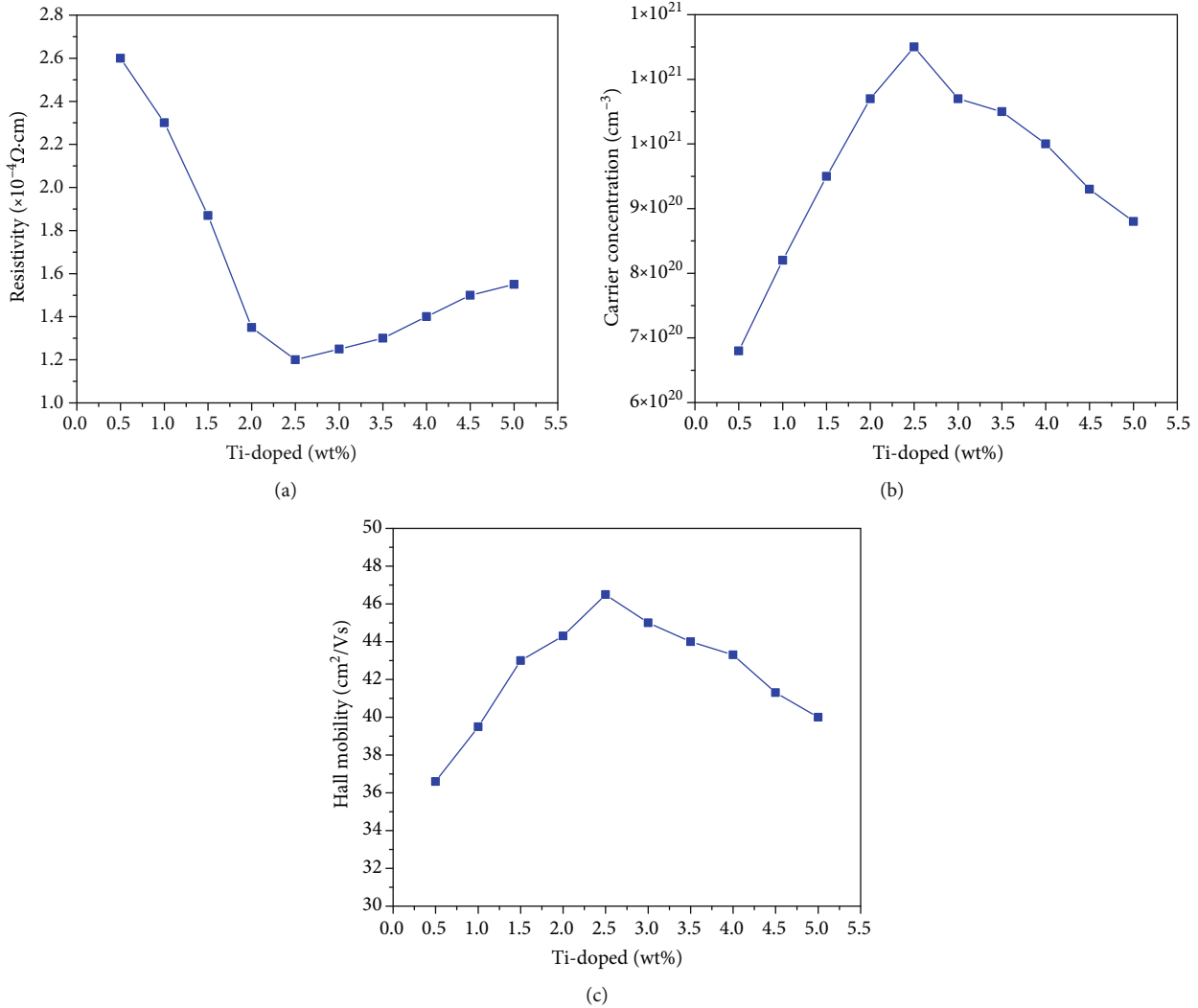


FIGURE 5: Overall variation in the electrical properties of the deposited films of different Ti doping concentrations: (a) resistivity; (b) carrier concentration; (c) Hall mobility.

TABLE 2: Comparison the electrical properties of the ITiO obtained from study to those of the films deposited by other processes.

Deposited methods of ITiO films	Substrate temperature (°C)	Resistivity (Ωcm)	Mobility ($\text{cm}^2/\text{V}\cdot\text{s}$)	Carrier concentration (cm^{-3})	References
Without oxygen atmosphere	300	—	27.5	8.82×10^{18}	[19]
RF magnetron sputtering (influence of RF power conditions)	400	1.2×10^{-4}	45.5	1.2×10^{21}	[20]
Pulsed DC magnetron sputtering	450	1.4×10^{-3}	64	7.1×10^{19}	[28]
Oxygen plasma treatment (PET substrate)	130	7.81×10^{-1}	—	—	[29]
RF magnetron sputtering (influence of Ti doping concentration)	300	1.14×10^{-4}	46.03	1.15×10^{21}	This study

Likewise, α can be calculated by using transmittance (T) (Figure 6) following [34]

$$\alpha = \frac{1}{d} \ln \left(\frac{1}{T} \right), \quad (3)$$

where d is the film thickness. Therefore, E_g can be gotten from plotting $\alpha h\nu$ in the function of $h\nu$ (according to Equation (1)). As an experimental result, the E_g values in the range from 2.73 eV to 3.57 eV were found (see Table 2). Table 3 presents the values of the optical band gap for the ITiO films.

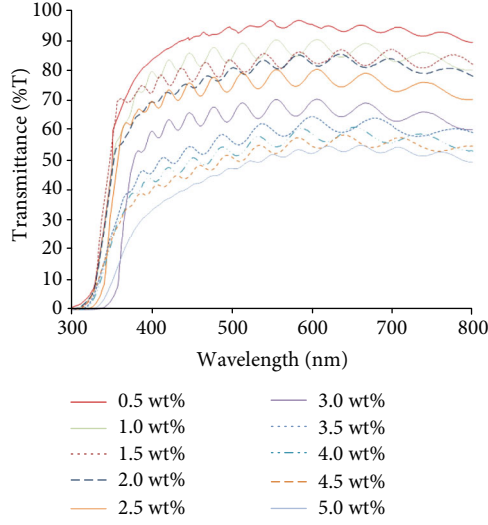


FIGURE 6: Optical transmittance of the deposited ITiO films of different doping concentrations from Ti-0.5 wt% to Ti-5.0 wt%.

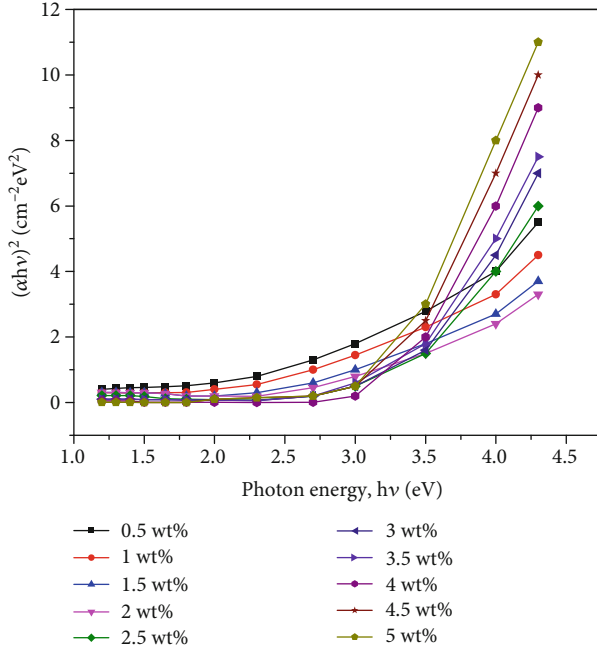


FIGURE 7: The $(\alpha h v)^2$ against photon energy ($h v$) of the deposited ITiO films of different doping concentrations from Ti-0.5 wt% to Ti-5.0 wt%.

TABLE 3: Energy gap (E_g) of ITiO films at the temperature of 300°C.

Ti (wt%)	0.5	1.0	1.5	2.0	2.5	3.0	3.5	4.0	4.5	5.0
E_g (eV)	2.73	2.79	2.85	2.97	3.18	3.22	3.29	3.35	3.42	3.57

In general, the E_g value of the present ITiO films has been gradually increased with a rise in the Ti content.

Moreover, we investigated the luminance properties of the ITiO films under different conditions of doping concen-

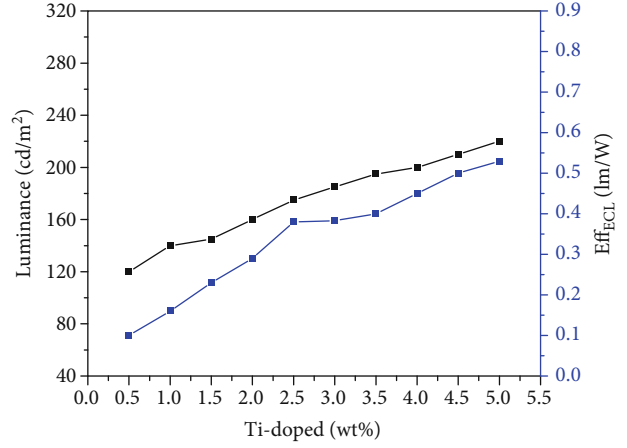


FIGURE 8: The luminance and ECL efficiency of the deposited ITiO films' different doping concentrations from Ti-0.5 wt% to Ti-5.0 wt%.

tration from 0.5 wt% to 5.0 wt%. As presented in Figure 8, the luminance trend has been gradually increased. We found that the maximum luminance was shown by a Ti content of 5.0 wt% (225.63 cd·m⁻²). The reason for the increased luminance was because the ITiO electrode has many electrons on its surface area which could have led to a faster transfer of electron and resulted in electron collision. This case is considered a crucial factor in the behavior of voltage waveform and faradaic current that affect the Ru(II) complex to charge the current on the ITiO film surface [35, 36]. However, according to Figure 5, their Ti content of 5.0 wt% presented a low electrical property. In order to obtain an effective electrical property, 2.5 wt% of Ti concentration was particularly considered because this condition illustrated good electrical qualities: the lowest resistivity and highest mobility and carrier concentration. Consequently, it can be clearly seen that Ti content 2.5 wt% presented the luminance value of 170.74 cd·m⁻². Additionally, the Eff_{ECL} presented in Figure 8 performed a light intensity per electrical power (lm/W). In general, there has been a steady rise of the Eff_{ECL} trend. Nevertheless, as mentioned earlier, at 2.5 wt% of Ti concentration, a good electrical property was displayed, showing an Eff_{ECL} value of 0.43 lm·W⁻¹ [37–39]. This can therefore be explained by the increasing number of the electrons on width surface causing a fast transfer electron [36, 40] with the higher Eff_{ECL} cell.

4. Conclusions

In this study, we have investigated the characteristic film properties of the ITiO films with the different doping concentrations deposited by using the RF magnetron sputtering method. The experimental results have shown that the average roughness (RMS) of ITiO films is sensitive to the doping concentration. As a result, the results show a great influence on the structural, morphological, electrical, and optical properties together with ECL efficiency on the ITiO films. The lowest resistivity of $1.14 \times 10^{-4} \Omega \text{cm}$ with the most intense XRD peak was also observed in Ti-2.5 wt%. Moreover, the transmittance and energy gap were

increased with the rising Ti content, especially when Ti-2.5 wt% has values of 82% in the wavelength range of the visible spectrum and 3.18 eV of energy gap along with the luminance and ECL efficiency of $170.74 \text{ cd}\cdot\text{m}^{-2}$ and $0.43 \text{ lm}\cdot\text{W}^{-1}$, respectively. Therefore, the obtained result has proven to be effectively responsible for preparing ITiO thin films with simultaneous improvement of effective good films where the feasibility of the ITiO films can be used as a transparent device application.

Data Availability

The data used to support the findings of this study are available from the corresponding author upon request.

Conflicts of Interest

The authors declare that there is no conflict of interest regarding the publication of this paper.

Acknowledgments

This work was supported by the Petchra Pra Jom Klaow Master's Degree Scholarship from King Mongkut's University of Technology Thonburi (KMUTT), Thailand (grant number 11, 2019), and under the project of the Research, Innovation, and Partnerships Office (RIPo) and National Research University Project of Thailand's Office of the Higher Education.

References

- [1] W. He and C. Ye, "Flexible transparent conductive films on the basis of Ag nanowires: design and applications: a review," *Journal of Materials Science & Technology*, vol. 31, no. 6, pp. 581–588, 2015.
- [2] U. Betz, M. Kharrazi Olsson, J. Marthy, M. F. Escolá, and F. Atamny, "Thin films engineering of indium tin oxide: large area flat panel displays application," *Surface and Coatings Technology*, vol. 200, no. 20-21, pp. 5751–5759, 2006.
- [3] K. Schulze, B. Maennig, K. Leo et al., "Organic solar cells on indium tin oxide and aluminum doped zinc oxide anodes," *Applied Physics Letters*, vol. 91, no. 7, article 073521, 2007.
- [4] D. Arai, M. Kondo, and A. Matsuda, "Reduction of light-induced defects by nano-structure tailored silicon solar cells using low-cost TCO substrates," *Solar Energy Materials and Solar Cells*, vol. 90, no. 18-19, pp. 3174–3178, 2006.
- [5] M. M. Richter, "Electrochemiluminescence (ECL)," *Chemical Reviews*, vol. 104, no. 6, pp. 3003–3036, 2004.
- [6] A. J. Bard and L. R. Faulkner, *Electrochemical Methods Fundamentals and Applications*, Wiley, New York, 2001.
- [7] J. J. Lin and Z. Q. Li, "Electronic conduction properties of indium tin oxide: single-particle and many-body transport," *Journal of Physics: Condensed Matter*, vol. 26, no. 34, p. 343201, 2014.
- [8] T. Hino, Y. Ogawa, and N. Kuramoto, "Preparation of functionalized and non-functionalized fullerene thin films on ITO glasses and the application to a counter electrode in a dye-sensitized solar cell," *Carbon*, vol. 44, no. 5, pp. 880–887, 2006.
- [9] G. Bernardo, G. Gonçalves, P. Barquinha et al., "Polymer light-emitting diodes with amorphous indium-zinc oxide anodes deposited at room temperature," *Synthetic Metals*, vol. 159, no. 11, pp. 1112–1115, 2009.
- [10] M. F. A. M. van Hest, M. S. Dabney, J. D. Perkins, D. S. Ginley, and M. P. Taylor, "Titanium-doped indium oxide: a high-mobility transparent conductor," *Applied Physics Letters*, vol. 87, no. 3, article 032111, 2005.
- [11] E. Peláez-Abellán, L. T. Duarte, S. R. Biaggio, R. C. Rocha-Filho, and N. Bocchi, "Modification of the titanium oxide morphology and composition by a combined chemical-electrochemical treatment on cp Ti," *Materials Research*, vol. 15, no. 1, pp. 159–165, 2012.
- [12] M. R. M. Marinho, T. M. Maciel, W. B. Castro, E. O. Almeida, and C. Alves Jr., "Deposition of thin film of titanium on ceramic substrate using the discharge for hollow cathode for $\text{Al}_2\text{O}_3/\text{Al}_2\text{O}_3$ indirect brazing," *Materials Research*, vol. 12, no. 4, pp. 419–422, 2009.
- [13] P. H. C. Camargo, K. G. Satyanarayana, and F. Wypych, "Nanocomposites: synthesis, structure, properties and new application opportunities," *Materials Research*, vol. 12, no. 1, pp. 1–39, 2009.
- [14] J. Meyer, P. Görrn, S. Hamwi, H. H. Johannes, T. Riedl, and W. Kowalsky, "Indium-free transparent organic light emitting diodes with Al doped ZnO electrodes grown by atomic layer and pulsed laser deposition," *Applied Physics Letters*, vol. 93, no. 7, article 073308, 2008.
- [15] S. Parthiban, K. Ramamurthi, E. Elangovan, R. Martins, E. Fortunato, and R. Ganeshan, "High-mobility molybdenum doped indium oxide thin films prepared by spray pyrolysis technique," *Materials Letters*, vol. 62, no. 17-18, pp. 3217–3219, 2008.
- [16] A. Valentini, F. Quaranta, M. Penza, and F. R. Rizzi, "The stability of zinc oxide electrodes fabricated by dual ion beam sputtering," *Journal of Applied Physics*, vol. 73, no. 3, pp. 1143–1145, 1993.
- [17] W. Yang, Z. Liu, D. L. Peng et al., "Room-temperature deposition of transparent conducting Al-doped ZnO films by RF magnetron sputtering method," *Applied Surface Science*, vol. 255, no. 11, pp. 5669–5673, 2009.
- [18] A. Martín, J. P. Espinós, A. Justo, J. P. Holgado, F. Yubero, and A. R. González-Elipe, "Preparation of transparent and conductive Al-doped ZnO thin films by ECR plasma enhanced CVD," *Surface and Coating Technology*, vol. 151–152, pp. 289–293, 2002.
- [19] C. J. Dong, W. X. Yu, M. Xu et al., "Significant effect of oxygen atmosphere on the structure, optical and electrical properties of Ti-doped In_2O_3 transparent conductive thin films," *Optica Applicata*, vol. 41, no. 3, 2011.
- [20] A. Chaoumead, H. D. Park, B. H. Joo, D. J. Kwak, M. W. Park, and Y. M. Sung, "Structural and electrical properties of titanium-doped indium oxide films deposited by RF sputtering," *Energy Procedia*, vol. 34, pp. 572–581, 2013.
- [21] Y. Abe and N. Ishiyama, "Titanium-doped indium oxide films prepared by d.c. magnetron sputtering using ceramic target," *Journal of Materials Science*, vol. 41, no. 22, pp. 7580–7584, 2006.
- [22] D. W. Han, J. Darma, E. Kuantama, D. J. Kwak, and Y. M. Sung, "Titanium-doped indium oxide films prepared by RF magnetron sputtering," in *2008 23rd International Symposium on Discharges and Electrical Insulation in Vacuum*, vol. 2, pp. 599–602, Bucharest, Romania, September 2008.

- [23] J.-H. Heo, K.-Y. Jung, D.-J. Kwak, D.-K. Lee, and Y.-M. Sung, “Fabrication of titanium-doped indium oxide films for dye-sensitized solar cell application using reactive RF magnetron sputter method,” *IEEE Transactions on Plasma Science*, vol. 37, no. 8, pp. 1586–1592, 2009.
- [24] D. J. Kwak, M. W. Park, and Y. M. Sung, “Discharge power dependence of structural and electrical properties of Al-doped ZnO conducting film by magnetron sputtering (for PDP),” *Vacuum*, vol. 83, no. 1, pp. 113–118, 2008.
- [25] W. J. Choi, B. H. Moon, T. W. Kim, S. H. Park, and Y. M. Sung, “Ti film deposition for fabrication of transparent conductive oxide less electrochemical luminescence cell,” *International Council on Electrical Engineering*, vol. 1, no. 4, pp. 1441–1445, 2014.
- [26] J. M. Bennett and L. Mattson, *Introduction to Surface Roughness and Scattering*, Optical Society of America, Washington DC, 1989.
- [27] S. M. Ali, S. T. Hussain, S. A. Bakar, J. Muhammad, and N. u. Rehman, “Effect of doping on the structural and optical properties of SnO_2 thin films fabricated by aerosol assisted chemical vapor deposition,” *Journal of Physics: Conference Series*, vol. 439, article 012013, 2013.
- [28] B. Grew, J. W. Bowers, F. Lisco, N. Arnou, J. M. Walls, and H. M. Upadhyaya, “High mobility titanium-doped indium oxide for use in tandem solar cells deposited via pulsed DC magnetron sputtering,” *Energy Procedia*, vol. 60, pp. 148–155, 2014.
- [29] S. Arunrungrusmi, P. Chansri, and N. Mungkung, “Transparent ITiO film electrodes on polyethylene terephthalate by oxygen plasma treatment for high-performance flexible electroluminescence device,” *Japanese Journal of Applied Physics*, vol. 58, no. SA, article SAAB02, 2019.
- [30] K. Ellmer, “Past achievements and future challenges in the development of optically transparent electrodes,” *Nature Photonics*, vol. 6, no. 12, pp. 809–817, 2012.
- [31] F. K. Shan, B. I. Kim, G. X. Liu et al., “Blueshift of near band edge emission in Mg doped ZnO thin films and aging,” *Journal of Applied Physics*, vol. 95, no. 9, pp. 4772–4776, 2004.
- [32] A. P. Amalathas and M. M. Alkaisi, “Effects of film thickness and sputtering power on properties of ITO thin films deposited by RF magnetron sputtering without oxygen,” *Journal of Materials Science: Materials in Electronics*, vol. 27, no. 10, pp. 11064–11071, 2016.
- [33] C. H. Huang, G. Zhang, Z. Q. Chen, X. J. Huang, and H. Y. Shen, “Calculation of the absorption coefficients of optical materials by measuring the transmissivities and refractive indices,” *Optics & Laser Technology*, vol. 34, no. 3, pp. 209–211, 2002.
- [34] D. J. Kwak, J. H. Kim, B. W. Park, Y. M. Sung, M. W. Park, and Y. B. Choo, “Growth of ZnO:Al transparent conducting layer on polymer substrate for flexible film typed dye-sensitized solar cell,” *Current Applied Physics*, vol. 10, no. 2, pp. S282–S285, 2010.
- [35] N. Itoh, “Electrochemical light-emitting gel made by using an ionic liquid as the electrolyte,” *Journal of the Electrochemical Society*, vol. 156, no. 2, pp. j37–j40, 2009.
- [36] W. Kaiser, R. P. Marques, and A. F. Correa, “Light emission of electroluminescent lamps under different operating conditions,” *IEEE Transactions on Industry Applications*, vol. 49, no. 5, pp. 2361–2369, 2013.
- [37] H. D. Park, Y. M. Sung, M. W. Park, and J. E. Song, “Comparison of electrochemical luminescence characteristics of titanium dioxide films prepared by sputtering and sol-gel combustion methods,” *Japanese Journal of Applied Physics*, vol. 52, no. 5S2, article 05EC04, 2013.
- [38] P. Chansri and Y. M. Sung, “Synthesis and characterization of TiO₂on ZnO-nanorod layer for high-efficiency electrochemiluminescence cell application,” *Japanese Journal of Applied Physics*, vol. 55, no. 2S, article 02BB11, 2016.
- [39] P. Chansri and Y. M. Sung, “Investigations of electrochemical luminescence characteristics of ZnO/TiO₂ nanotubes electrode and silica-based gel type solvents,” *Surface and Coating Technology*, vol. 294, pp. 220–224, 2016.
- [40] C. Zhang, B. Qiao, S. Zhao et al., “Transient analysis on stored charges in organic light-emitting diodes and their application in alternating current driven electroluminescence,” *Organic Electronics*, vol. 39, pp. 348–353, 2016.